

## Chapter 5 Development of a Biodegradable Microfluidic Paper-based Device for Blood-plasma Separation Integrated with Non-enzymatic Electrochemical Detection of Ascorbic Acid

---

---

### 5.1 Overview

In this chapter, we have developed an electrochemical microfluidic paper-based device (E $\mu$ PAD) for the non-enzymatic detection of Ascorbic Acid (AA) concentration in plasma using whole human blood. We combined LF1 blood plasma separation membrane and Whatman grade 1 filter paper to separate plasma from whole blood through wax printing. A screen-printed-electrode (SPE) was modified with spherical-shaped MgFe<sub>2</sub>O<sub>4</sub> nanomaterial (n-MgF) to improve the catalytic properties of SPE. The n-MgF was prepared via hydrothermal method, and its material phase and morphology were confirmed via XRD, FTIR, TEM, SEM, and AFM analysis. The fabricated n-MgF/SPE/E $\mu$ PAD exhibited detection of AA ranging from 0 to 80  $\mu$ M. The obtained value of the detection limit, limit of quantification, sensitivity, and response time are 2.44  $\mu$ M, 8.135  $\mu$ M,  $5.71 \times 10^{-3}$  mA  $\mu$ M<sup>-1</sup> cm<sup>2</sup>, and 10 seconds, respectively. Our developed n-MgF/SPE/E $\mu$ PAD shows marginal interference with the common analytes present in plasma, such as uric acid, glutamic acid, glucose, urea, lactic acid, and their mixtures. Overall, our low-cost, portable device with its user-friendly design and efficient plasma separation capability offers a practical and effective solution for estimating AA concentration from whole human blood in a single step.

## 5.2 Introduction

Blood test is the first step toward analysing the infection present in human body. However, RBCs present in blood sample interfere with the other analytes and mislead the results. In order to quantify analytes, present in the blood plasma, the first step is to separate plasma from whole human blood. Clinically, centrifugation method has been utilised to separate plasma from whole blood [148]. However, centrifugation method is time consuming and requires a large volume of blood sample. Alternatively, microfluidic paper-based platform can separate plasma from whole human blood within one to two minutes with 98% accuracy [131]. Paper-based microfluidic analytical devices ( $\mu$ PADs) have gained immense interest during the last decade due to their many advantageous features, including self-pumping, low sample volume requirements, rapid analysis, high sensitivity, reduced sample handling, miniaturization, biodegradable, and reduced cost. Recently, Whiteside's group has reported  $\mu$ PAD as an alternative technique for point-of-care setting in developing countries [149]. Several methods are available to fabricate  $\mu$ PAD such as photolithography [149], plasma treatment [26], polydimethylsiloxane (PDMS) plotting [13], inkjet printing [24], wax screen printing [150] and wax dipping [151]. The selection of correct fabrication method depends on the specific type and complexity of the device used for production. In  $\mu$ PAD due to capillary action fluid moves through the hydrophilic zone circumventing its movement in hydrophobic regions. In the present scope of work wax dipping method was used to create a microfluidic channel having a combination of blood filter membrane (LF1) and Whatman grade 1 filter paper to separate plasma from whole blood sample. Paper-based devices for analyte detection generally use one of the two methods: colorimetric [152] or electrochemical [153]. Colorimetric methods rely on a change in color on the paper surface confirming the presence of the analyte, while electrochemical methods use electrical signal generated due to redox reaction leading to the detection of such analyte. The most popular method of detection is colorimetric, it either

employs a chemical or an enzymatic reaction to provide a color change in hydrophilic region. The color intensity is proportional to the analyte concentration for the quantification of the analyte concentration and smart phone, scanner or digital camera is used to measure the color intensity [18]. However, errors in color intensity measurement occur due to paper background color, background light, and non-uniform mobility of fluid on porous paper surface which develop uneven color change. To overcome such issues electrochemical approaches have been employed in preference to classical colorimetric approaches.

However, electrochemical techniques have become increasingly popular due to their ability to provide fast results and high level of sensitivity. In the realm of electrochemical sensors screen-printed-electrode (SPE) have become particularly popular because they offer numerous benefits over conventional three electrode systems such as low cost, ability to be miniaturized, ease of use, high level of reproducibility, versatility in applications, low background current, and stability [154] [155]. In general, the utilization of SPEs prove to be advantageous in several areas such as analytical chemistry, bio sensing, and other related fields [156] [157].

The SPE consists of three electrodes (counter, reference, and working) that facilitate oxidation-reduction reactions and produce an electrochemical signal proportional to the concentration of analyte present in solution [158]. The working electrode is typically prepared using carbon ink, which may contain some non-conductive substances that reduce its sensitivity and selectivity towards electrochemical detection. To improve the electrochemical performance of the SPE, nanomaterials can be utilized to modify the working electrode. Nanomaterials possess unique properties, such as large surface area, small size, quantum effects, that enhance sensitivity, selectivity, and stability of SPE [159], [160], [161]. Metal or metal oxide nanomaterials can be used to enhance the catalytic activity of SPE towards the detection of specific analytes such as Ascorbic Acid, dopamine, and uric acid [162], [163], [164]. In the present scope of research metal ferrite modified SPE has been utilised to detect Ascorbic Acid (AA) in real whole blood

sample. AA, also known as Vitamin C is an essential water-soluble vitamin and has a significant role in the biological mechanism of human body. AA participates in various physiological and biochemical reaction mechanisms such as the maintenance of blood vessels, the absorption of metal ions, the acceleration of collagen production, and the release of the adrenal gland [165]. Furthermore, free radicals scavenging capacity of AA helps in preserving the balance of oxidation and reduction in human tissue [166]. The concentration of AA in human plasma typically lies within the range of 33  $\mu\text{M}$  to 111  $\mu\text{M}$  [167]. A concentration of AA below the clinical range causes serious diseases such as scurvy, cancer, Alzheimer, Parkinson, and cardiovascular disorders [168]. On the other hand, an excess amount of AA causes stomach cramps, urinary stones, and diarrhoea [169]. Therefore, measuring AA levels is a vital diagnostic factor that offers essential insights into overall health of an individual.

Several nanomaterial grafted SPE has already been reported to detect the AA concentration in food, urine, and plasma samples [162], [163], [164], [170], [171], [172], [173]. Most of these modified SPE having following disadvantages such as poor detection limit, not cover physiological range of AA human plasma, poor sensitivity, high response time etc. A comparison table was constructed between the performance parameter obtained from our developed device and previously reported modified SPEs to measure the AA concentration (Section 3.5). Recent study suggest that, ferrite nanomaterials, which are a type of ceramic materials consisting of iron oxide and other metal oxides, are often used to modify the working area of SPEs for various electrochemical applications [162]. Ferrite nanomaterials have high magnetic and catalytic properties that enhance the electrochemical performance of the SPEs [174]. Spinel ferrite nanomaterial, such as cobalt ferrite ( $\text{CoFe}_2\text{O}_4$ ) and nickel ferrite ( $\text{NiFe}_2\text{O}_4$ ), have been used to modify SPEs for the detection of hydrogen peroxide, glucose, and other analytes [175], [176]. The high surface area and catalytic activity of these materials can improve the sensitivity and selectivity of the SPEs towards the target analytes. Among the

various available metal ferrites, magnesium ferrite nanomaterial (n-MgF) has been used in the present work to modify the working area of SPEs for analyte detection due to its following features: (a) n-MgF exhibits high catalytic activity towards the electrochemical oxidation of analyte improving the sensitivity and selectivity of the SPEs towards the target analytes, and (b) n-MgF is stable and durable under various environmental conditions, including change in pH and temperature [177]. The stability and durability of n-MgF enhance the performance of the modified SPEs. Additionally, these nanoparticles have been found to be biocompatible, which makes them suitable for bio sensing applications. Furthermore, these nanoparticles can easily be synthesized using low-cost precursors and simple synthetic routes, which makes them a cost-effective and practical option for SPE modification.

The integration of paper-based devices with SPEs offers several advantages. The small size and portability of both paper-based devices and SPEs make them ideal candidates for using in field applications as well as point-of-care (POC) diagnostics [178]. SPEs are highly sensitive to change in the electrochemical properties of the sample, while paper-based devices can provide high surface area for the immobilization of biomolecules, leading to highly sensitive and specific detection [179]. Blood plasma separation occurs on the  $\mu$ PAD simultaneously without the intervention of any external force. Thus, the integration of paper-based devices with SPEs allows for fast and automated analysis, making them ideal for high-throughput screening [180]. Electrochemical microfluidic paper-based analytical device ( $E\mu$ PAD) provide selective and ultrafast detection within nM concentration range of analyte [139]. It is also worthy to mention that in this study  $\mu$ PAD is used to facilitate plasma separation from whole human blood. In the present scope of work n-MgF modified SPE integrated with  $\mu$ PAD has been utilised to detect the Ascorbic Acid (AA) concentration in plasma.

In this article an electrochemical microfluidics paper-based device ( $E\mu$ PAD) has been developed for AA detection in plasma (output) using whole blood sample (input). In the first

part of the work blood filter membrane (LF1) is combined with Whatman grade 1 filter paper via green wax dipping technique to separate plasma from whole blood. For electrochemical sensor development, SPE working area is modified with n-MgF utilising drop casting method to improve the catalytic behaviour and selectivity of the SPE towards AA detection. The n-MgF was synthesized through hydrothermal route and all material characterisation such as FTIR, XRD, SEM, TEM, and AFM were performed. All electrochemical characterisation were also investigated for the performance analysis of n-MgF/SPE. The developed E $\mu$ PAD covers the entire clinical range of AA available in human plasma sample along with that having high detection limit (LD), excellent sensitivity, and quick response time. To the best of our knowledge, in the current state of the art, n-MgF/SPE integrated with  $\mu$ PAD for AA detection using whole blood sample has not yet been reported. In a nutshell, existing literature does not provide a miniaturized ultrafast device for accurate estimation of ascorbic acid in simple-in answer-out format which motivates the authors to develop such low-cost clinical assay to be easily deployed in fields.

## 5.3 Experiment

### 5.3.1 Chemical and materials

Mg(NO<sub>3</sub>)<sub>2</sub>.6H<sub>2</sub>O, Fe(NO<sub>3</sub>)<sub>3</sub>.9H<sub>2</sub>O, NH<sub>3</sub> (25% solution), were purchased from Merck Mumbai. Olive oil (Figaro, from local market Varanasi), Whatman no-1 filter paper, LF1 membrane, and Ascorbic acid were procured from sigma Aldrich Germany. NaH<sub>2</sub>PO<sub>4</sub>.2H<sub>2</sub>O (sodium dihydrogen phosphate dihydrate, 99%), Na<sub>2</sub>HPO<sub>4</sub>.2H<sub>2</sub>O (disodium hydrogen phosphate dihydrate, 99%), K<sub>3</sub>(Fe(CN)<sub>6</sub>) potassium hexacyano-ferrate (III) (98.5%) and K<sub>4</sub>(Fe(CN)<sub>6</sub>).3H<sub>2</sub>O, potassium hexacyanoferrate (II) trihydrate and NaCl (99%) were purchased from Merck,

Mumbai, India. SPE purchased from PalmSens. Iron sheets of 10×10 cm were purchased from local market of Varanasi. Wax was purchased from Merck ([www.merckmillipore.com](http://www.merckmillipore.com)).

### 5.3.2 Instruments

The phase and crystallinity of the n-MgF powder was measured using a D8 Advance diffractometer (Bruker) with X-ray source used as a CuK $\alpha$  ( $\lambda = 1.54\text{\AA}$ ) using X-ray diffraction (XRD) technique in the range of 20 to 70° with step size of 0.03°. FTIR spectra of n-MgF was recorded in the range of 4000-650 cm<sup>-1</sup> by using PerkinElmer spectrometer. Transmission electron microscopy (TEM) (Technai G20) was used to study the morphology of n-MgF. Scanning electron microscopy (SEM) (CARL ZEISS MICROSCOPY LTD,) was used to confirm the surface morphology of n-MgF. Atomic force microscopy (AFM) NT-MDT Service & Logistics Ltd, was used to check the surface roughness of n-MgF/SPE. A computer-controlled electrochemical analyzer Corrtest CS studio-350 was used for all electrochemical measurements. A standard screen-printed three-electrode setup was used in which carbon as the working electrode (area = 0.707 cm<sup>2</sup>), carbon as the counter electrode, and Ag/AgCl as the reference electrode.

### 5.3.3 Blood Sample collection

Blood samples were obtained from the Sir Sunderlal hospital's surgical oncology division at BHU, Varanasi. K<sub>3</sub>EDTA tubes, which are often employed for anticoagulant causes, were used to ensure sufficient sample collection and handling. The use of K<sub>3</sub>EDTA helps keep blood from clotting and ensures that the integrity of the sample is maintained. The research examination obtained approval from an ethics committee before starting the sample collection process. This stage shows that ethical guidelines have been adhered to, assures that the study conforms to

proper procedures, and protects the rights and welfare of the participants. The experiment was conducted out within four hours following the sample collection in order to ensure the reliability and honesty of the samples which were assembled.

### **5.3.4 Microfluidic channel fabrication**

The microfluidic channel was fabricated by wax dipping method [11]. This method utilizes a dumbbell-shape mould, permanent magnets, glass slide, Whatman cellulose paper, LF1 membrane, and wax maintained at temperature 110-115 °C. The dumbbell shape mould was designed using AutoCAD software, and cut with Electrical Discharge Machining (Expresscut Series-Ex 4032C) from iron sheet. The prepared mould was further used to fabricate the microfluidics channels. The paper channel consists of three circular zones. The central circular zone was made of Whatman grade 1 filter paper for fast flow of plasma sample, and circular zone at both ends were prepared using LF1 membrane for sample inlet. The LF1 membrane hinders the red blood cells flow due to small pore diameter (0.45 µM) and only allows plasma to flow in lateral direction. All the three papers were overlapped to each other by 1 mm from edges and kept on a clean glass slide (*Figure 5.1(C)*). The iron mould was then kept over the top of the paper assembly and a magnetic bar was placed at the bottom of the glass slide (*Figure 5.1(e)*). The magnetic bar applied a strong magnetic force over the iron mould, which minimise the gap between iron mould and paper surface. The whole assembly was then dipped into a wax container maintained at a temperature of 110-115 °C (*Figure 5.1(f)*) for 1 second [11]. Further, the assembly was allowed to cool at room temperature to solidify the wax and iron mould was removed. Finally, a microfluidic channel was obtained which having combination of both LF1 membrane and Whatman grade 1 filter paper. This prepared microfluidic channel is biodegradable and the iron mould can be used 1000 times for further fabrication process.

The schematic representation of steps involved in the fabrication of microfluidic channel are depicted in *Figure 5.1*.

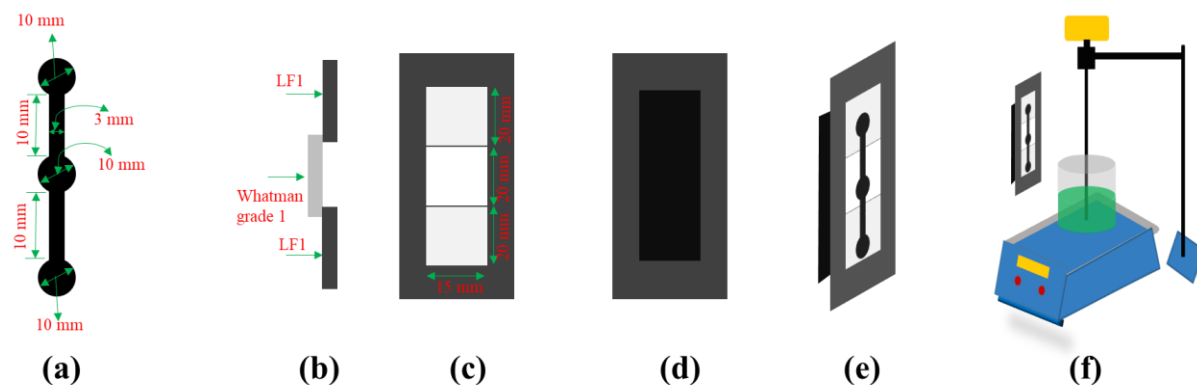


**Figure 5.1** Schematic representation of wax dipping method to develop microfluidic channel. (a) Dumbbell shape iron mould for microfluidic channel fabrication (b) Side view of LF1 and Whatman grade 1 filter paper assembly (c) Top view of filter paper assembly kept on a glass slide (d) Permanent magnet attached at the back side of the glass slide (e) Dumbbell shape Iron mould kept at the top of the filter paper (f) Whole assembly dip inside the hot melted wax (110 °C) for 1 sec.

### 5.3.5 Material synthesis and SPE modification

n-MgF was prepared using hydrothermal synthesis method. 0.5 M  $\text{Mg}(\text{NO}_3)_2 \cdot 6\text{H}_2\text{O}$  salt and 1M  $\text{Fe}(\text{NO}_3)_3 \cdot 9\text{H}_2\text{O}$  salt were dissolved in 50 ml DI water. The solution was kept on magnetic stirring for 30 minutes. After that surfactant (olive oil) was added in the solution and drop wise ammonia solution was added to maintain the solution pH 10 at 60 °C, 800 rpm for additional 30 minutes. After this the solution was transferred into Teflon autoclave and kept inside a oven at 180 °C for 20 hours. The solution was left at room temperature to cool down and 6 to 7 time

washing was done using a mixture of DI and ethanol. The solution was collected in petri dish and dried at 90 °C for 10 hours. The dried sample was further calcinated at 600 °C for 4 hours. A dark brown color powder was obtained after grinding of the dried sample.

In the present scope of work a simple drop-casting method is utilized to modify the working electrode. 1 mg/ml solution of MgFe<sub>2</sub>O<sub>4</sub> nanomaterial powder were dispersed in DI water, which further kept for sonication at 25 minutes that properly disperse nanomaterial in DI water. This solution was further used to modify the working electrode of SPE. 10 μL of the solution was drop-casted over the working area and kept overnight at room temperature to dry the electrode shown in. The modified electrode was stored in a petri dish at room temperature for further applications. The outline of all the work is illustrated in *Figure 5.2*.

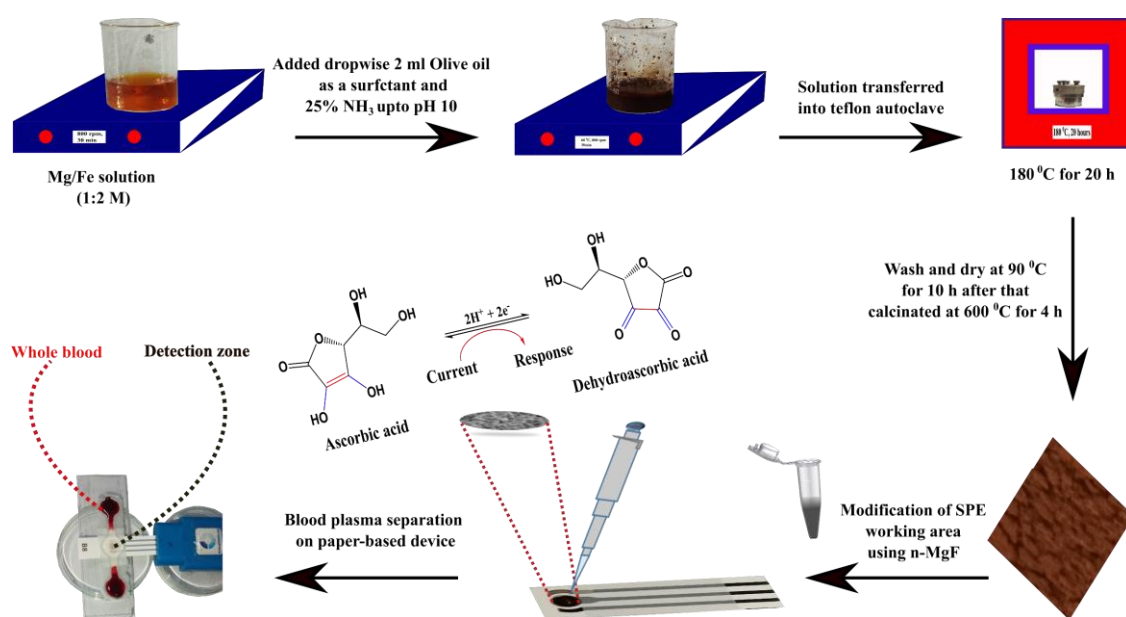


**Figure 5.2** Schematic representation of complete fabrication process of EμPAD from material synthesis to integration of microfluidic platform with n-MgF/SPE.

### **5.3.6 Measurement of AA using E $\mu$ PAD**

Initially modified n-MgF was attached with SPE holder in electrochemical transducer setup. After that, prepared microfluidics channel was kept on the top of modified n-MgF /SPE. The whole assembly was placed on a horizontal surface to maintain the uniform flow of blood-plasma sample shown in *Figure 5.2*. Whole blood samples were used for real sample analysis. Equal volume of whole blood was injected from both side of the dumbbell shaped reservoir and plasma separated from whole blood sample travelled to the detection zone. At the same time redox mediator was injected on the detection zone to measure the bioanalyte by electrochemical techniques. To maintain the uniformity in the experiment both calibration curve and real sample analysis were performed on microfluidic platform.

## **5.4 Results and discussion**

### **5.4.1 Microfluidic channel optimisation**

Here, a dumbbell shape microfluidics channel was selected that produced a consistent flow of plasma to the detection zone from both the ends. The middle section of the dumbbell had a diameter of 8.5 mm to accommodate the electrodes of SPE. Both inlet section had the same diameter of 12 mm to obtain a large amount of plasma at central zone. Additionally, dumbbell shape channel also balances the distribution of vertical forces throughout the microchannel along with conformal contact with SPE.

### 5.4.2 LF1 Membrane and sample volume optimisation data

LF1 membrane was used as a blood separation membrane in the present experiment. Here, first of all the volume of blood required to completely fill the detection zone with plasma was optimized. Initially, we had taken an undiluted blood sample (~ 50% Hematocrit (Hct)) of different volume (40, 50, 60, 70, 80, 90, and 100  $\mu\text{L}$ ) and injected from both inlet zones separately. We plotted the sample volume against time taken by plasma to completely fill detection zone, as shown in **Figure 5.3(a)**. It can be observed that the time taken by the plasma to reach the detection zone decreases with sample volume. However, in case of 90  $\mu\text{L}$  sample volume the red blood cells also start travelling along the plasma, which may consequently lead to the interference with the analyte's concentration. Therefore, 80  $\mu\text{L}$  sample volume injected from both sides separately was selected as an optimum sample volume to perform the experiment.

### 5.4.3 Time taken by various Hct sample to reach at detection zone

Further the experiment was conducted to observe the average time taken by separated plasma to reach up to detection zone when a fixed volumes (80  $\mu\text{L}$ ) of whole blood having different Hct were separately injected from both ends. It is clearly visible from **Figure 5.3(b)** that the maximum time of 240 second was taken by blood sample with Hct 55% and minimum time of 120 second was taken by blood sample with Hct 27% to completely fill the detection zone. The average time taken by prepared microfluidic channel to separate blood plasma is 2-4 minutes which is quite less compared to conventional blood plasma separation devices.

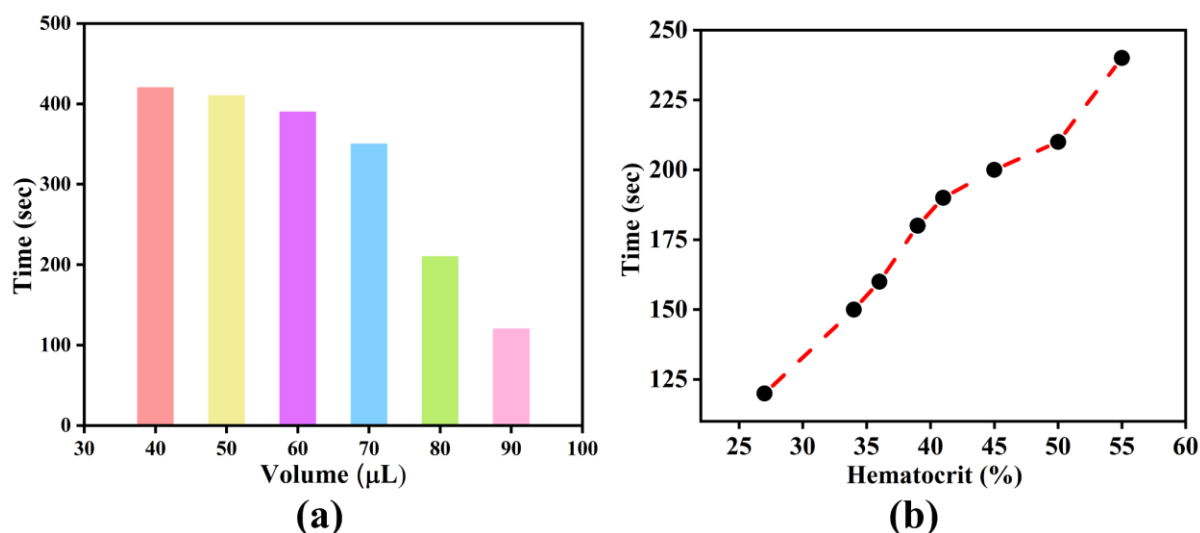


**Figure 5.3** (a) A bar graph between different volume of 50 % Hct blood sample injected from both ends and time taken by the plasma to completely fill the detection zone; (b) A line graph between a fixed volume (80  $\mu\text{L}$ ) of different Hct samples vs time taken by plasma to completely fill the detection zone.

#### 5.4.4 Material phase and morphology characterisation

n-MgF nanomaterial was synthesized using a simple hydrothermal technique and for various material characterisations such as FTIR, XRD, FESEM, and TEM. At first, FTIR spectroscopy was performed. FTIR provided the insights about molecular structure, chemical composition, and surface properties of nanomaterial. The FTIR absorption peaks were recorded in the range of 400 to 4000  $\text{cm}^{-1}$  wavenumber. The broad peak at 1384 and 1603  $\text{cm}^{-1}$  signifies the stretching vibration of  $\text{NO}_3^{-1}$  and O-H bending vibration [181]. As shown in **Figure 5.4(a)** two major peaks observed at 471 and 546  $\text{cm}^{-1}$  in fingerprint region, represents the stretching vibration of metal oxide bond at octahedral (Mg-O) and tetrahedral (Fe-O) sites, which confirms the successful formation of n-MgF [182].

X-ray diffraction (XRD) technique is utilised to study the crystalline nature and phase of the nanomaterial. XRD patterns for hydrothermally synthesized n-MgF were recorded in the  $2\theta$  range from  $20$  to  $80^\circ$  as depicted in **Figure 5.4(b)**. The XRD graph shows a diffraction at (220), (311), (400), (511), and (440) corresponding planes. The average crystallite size of n-MgF has been found as  $10.1035$  nm approximately using the well-known Scherrer's equation [183]. The crystalline structure of the nanomaterial was examined by comparing the position (diffraction angle) and lattice parameter ( $a$ ) of the diffraction peaks with the standard powder X-ray diffraction data. The value of the lattice parameter has been found as  $8.485 \text{ \AA}$  which exactly matches with JCPDS card no. 711232 confirming the formation of n-MgF nanomaterial in cubic system having FCC lattice with space group  $Fd\bar{3}m$  [227]. The abovementioned diffraction peak confirms the formation of n-MgF nanomaterial and validates the FTIR data.

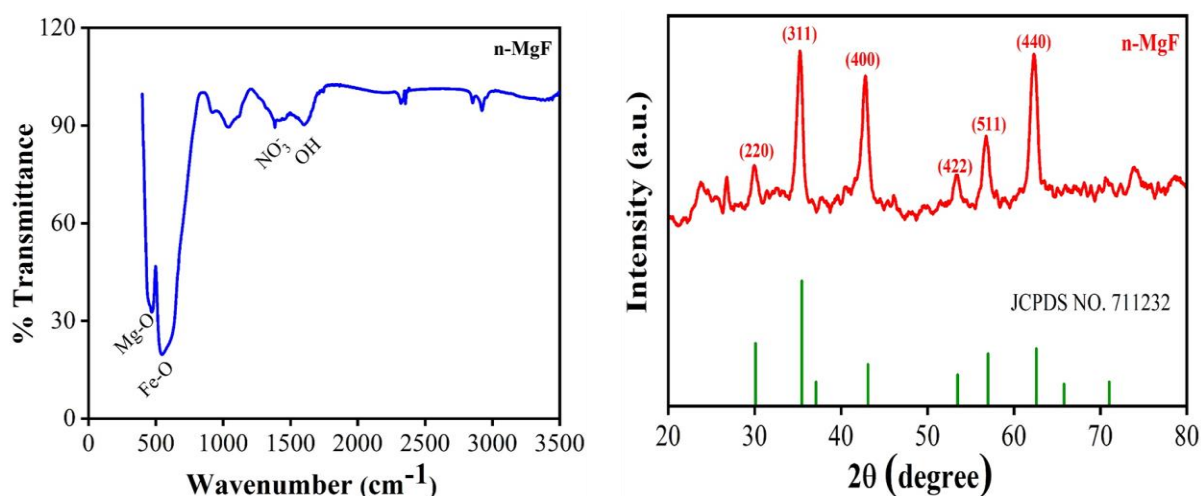


**Figure 5.4** (a) FTIR analysis of n-MgF: (b) XRD analysis of n-MgF.

The internal surface morphology of the n-MgF nanomaterial was further confirmed by TEM. The parallelogram morphology of the homogeneously distributed material was achieved after

TEM analysis as shown in **Figure 5.5(a)**. The average particle size of n-Mg has been found as 17 nm which was calculated from a histogram using Lorentzian function as shown in **Figure 5.5 (b)**. Furthermore, the selected area electron diffraction (SAED) image shows the interplanar spacing ( $d$  0.26, 0.21, and 0.14 nm) of the diffraction peak observed to the corresponding plane 311, 400, and 440 (**Figure 5.5(c)**). These results show good agreement with JCPDS card value of the  $d$ -spacing (0.25 nm) in the XRD analysis with respect to high intensity plane.

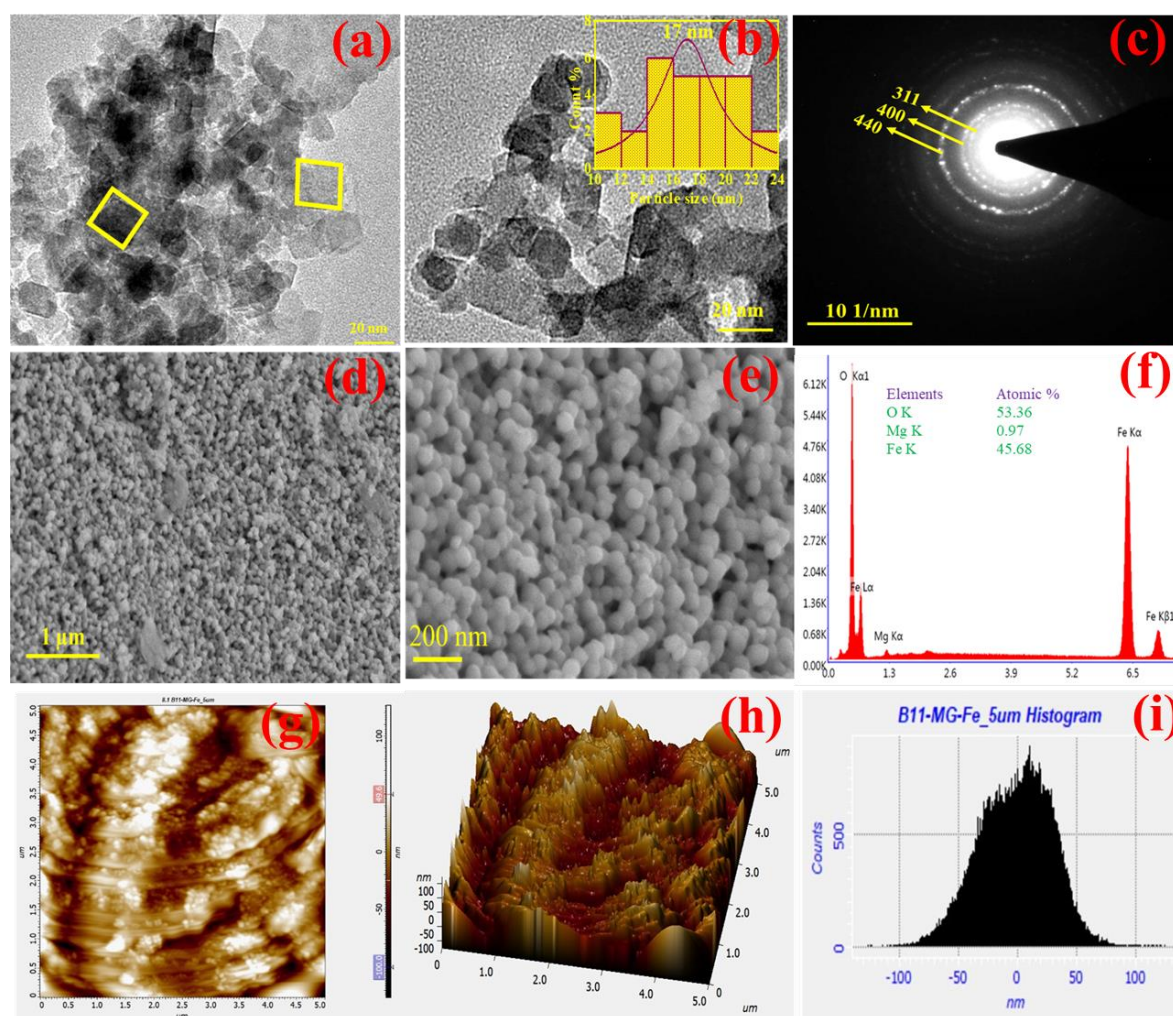


**Figure 5.5** Micrographs of TEM analysis of n-MgF (a), (b), and (c); SEM and EDX analysis of n-MgF (d), (e), and (f); AFM two dimensional (2D), three dimensional (3D), and roughness parameter analysis of n-MgF/SPE (g), (h), and (i).

The surface morphology of n-MgF was investigated through scanning electron microscopy (SEM) characterisation technique. A laser X-ray source of tungsten filament at 5 KV accelerating voltage was used for SEM analysis and prior to the experiment, sample was coated with gold metal using sputtering technique. **Figure 5.5**(d) and (e) indicate that the prepared n-MgF were arranged in a homogenous stratified microsphere like structure having a relatively rough surface of average diameter 73 nm. The EDX spectrum of the n-MgF verifies the presence of Fe (44.53%), Mg(1.36%), and O(54.11%) elements and further verify the formation of single phase n-MgF (**Figure 5.5**(f)).

Additionally, atomic force microscopy (AFM) was performed to investigate the surface roughness of n-MgF. **Figure 5.5**(g), (h), and (e) show the 2D and 3D micro-image of n-MgF distributed uniformly. The roughness parameter such as the average roughness ( $S_a$ ), root mean square roughness ( $S_q$ ), and maximum area peak height ( $S_p$ ) have been found as 24.6 nm, 30.191 nm, and 126.03 nm respectively on SPE surface. The average roughness is responsible for effective interaction with analyte in electrochemical sensing. All material characterisation results confirmed the successful formation of homogenous microsphere of n-MgF.

#### **5.4.5 Electrochemical analysis**

The electrochemical technique is effectively used to quantify the target analyte. In the present article, AA detection was carried out in whole blood sample and cyclic voltammogram (CV) analysis was performed for sensing. The electrochemical analysis of SPE and n-MgF/SPE were performed in a 50 mM phosphate buffer saline (PBS, 0.9% NaCl) solution containing 5mM ferri/ferro cyanide redox couple (FRC) at pH 6 with scan rate of 50 mV/s. It may be noted that all electrochemical optimization study were performed using standard PBS solution.

The CV response of SPE and n-MgF/SPE were recorded at a scan rate of 50 mV/s. As shown in **Figure 5.6(a)** oxidation peak current ( $I_{pa}$ ) value of SPE and n-MgF/SPE have been obtained as 0.0589 mA and 0.07167 mA at 0.26 V. The obtained value of  $I_{pa}$  for later case has been found to be higher due to electrostatic interaction of positive metal ion (Mg and Fe) with negative ion of FRC. The DPV response of the SPE and n-MgF/SPE was completely consistent with the CV results and suggested that the n-MgF improved the electron transport and electrocatalytic activity between the electrode and FRC (**Figure 5.7(a)**).

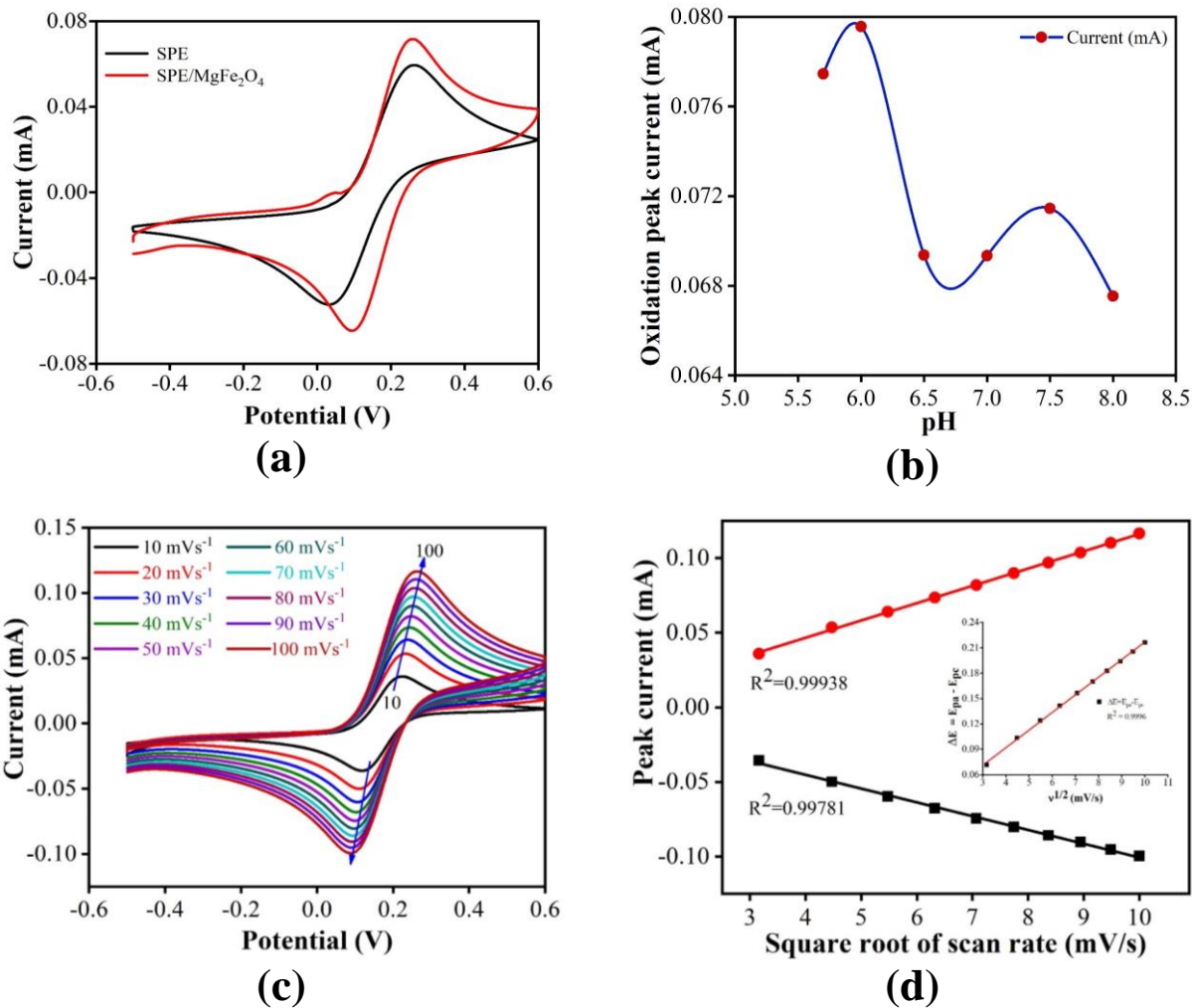


**Figure 5.6** CV analysis of unmodified SPE and n-MgF/SPE; (b) pH study of n-MgF/SPE; (c) Scan rate analysis of n-MgF/SPE for 10 to 100 scan rate; (d) peak current values plotted against the square root of the scan rate ( $v^{1/2}$ ).

In electrochemical biosensor, pH has a significant role for the detection of analyte. The optimum pH value of the n-MgF/SPE electrode was investigated by using CV technique in the pH range of 5.7 to 8 at 50 mV/s scan rate in standard PBS solution. As shown in **Figure 5.6(b)** I<sub>pa</sub> value increases in the pH range of 5.5 to 6 and after that I<sub>pa</sub> value starts reducing with pH. The modified n-MgFe/SPE has shown the maximum current intensity at pH 6 (0.079 mA)

indicating the highest interaction between electrode and FRC. Therefore, all other electrochemical analysis was performed at pH 6.

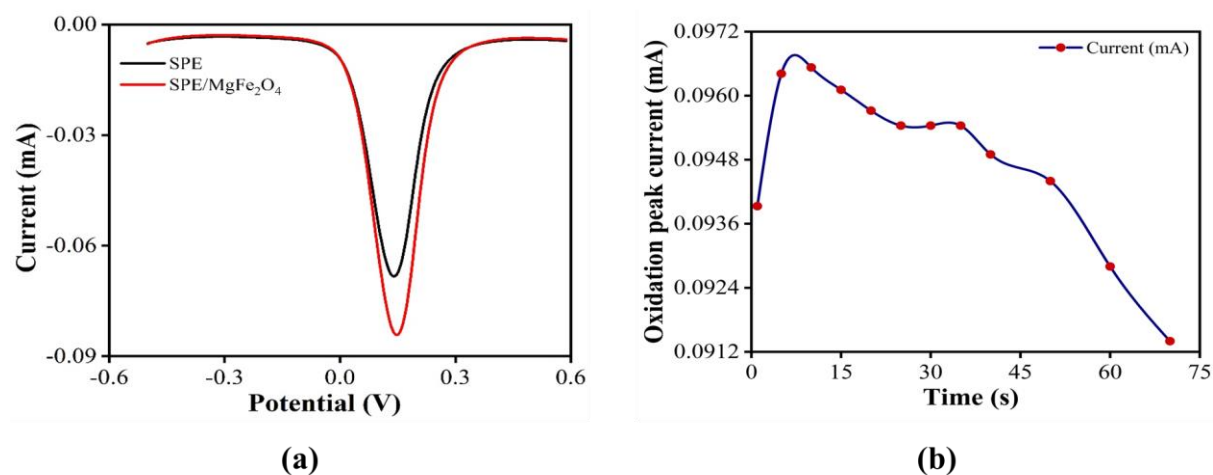


**Figure 5.7** DPV analysis of unmodified SPE and n-MgF/SPE; (b) Response time study of n-MgF/SPE.

Response time measurement is an important parameter for the development of electrochemical sensor. Response time of the modified electrode directly depends on the interaction between electrode and analyte interface. The response time measurement of the fabricated n-MgFe/SPE was carried out in standard PBS solution at 50 mV/s using 40  $\mu$ M standard AA for the range of 1 to 70 second with a regular interval of 5 second. The maximum value of  $I_{pa}$  (0.096 mA) was obtained for response time duration of 10 second (**Figure 5.7(b)**) which has consistently been used for further analysis.

The interfacial kinetics behaviour of the n-MgF/SPE were studied by recording CV response in standard PBS solution between 10 to 100 mV/s scan rates as depicted in **Figure 5.7(c)**. The current response of the electrode increases with increasing scan rate due to decrement of

diffusion layer in electrolytic solution [184]. The shifting of peak potential towards more positive and negative value supports the quasi-reversible nature of the interaction between electrode and electrolyte. In **Figure 5.7(d)** the peak current values plotted against the square root of the scan rate ( $v^{1/2}$ ) indicated that the oxidation peak current ( $I_{pa}$ ) and reduction peak current ( $I_{pc}$ ) increases linearly with  $v^{1/2}$ . The potential peak shift ( $\Delta E_p = E_{pa} - E_{pc}$ ) also exhibits a linear variation ( $R^2 = 0.99$ ) with  $v^{1/2}$  representing the diffusion-controlled interaction between electrode and electrolyte and shows the enhanced electrocatalytic behaviour of the electrode. The electron-transfer coefficient ( $K_s$ ) of n-MgFe/SPE is calculated using the following expression  $K_s = mnFv/RT$ , where  $m$  represents peak to peak separation (in V),  $n$  is number of electrons,  $F$  represents Faraday constant (96500 C/mol),  $v$  corresponds to scan rate,  $R$  is universal gas constant (8.314 J/mol/ K),  $T$  is the temperature (300 K) [185]. The estimated value of  $K_s$  has been found as  $0.30236 \text{ s}^{-1}$ , which reflects the enhanced catalytic activity and an increased rate of electron transfer of the n-MgF/SPE. Moreover, the electrode surface concentration ( $Y$ ) of n-MgF/SPE was calculated using Brown-Anson model ( $I_p = n^2F^2YA v/4RT$ ), where  $A$  is surface area of working electrode ( $0.70 \text{ cm}^2$ ) [186] where the calculated value of  $Y$  has been found as  $9.88622 \times 10^{-8} \text{ mol/cm}^2$ , indicating an enhanced electroactive surface area. Furthermore, Randles-Sevcik equation ( $I_p = (2.69 \times 10^5) n^{3/2} A D^{1/2} v^{1/2} C$ ), was used to estimate the diffusion coefficient ( $D$ ) value for diffusion process from electrolyte to electrode surface of n-MgF/SPE, where  $C$  indicates the mediator concentration ( $5 \times 10^{-6} \text{ mol-cm}^{-3}$ ). The calculated value of  $D$  has been found as  $0.0940 \text{ cm}^2/\text{s}$ . It is worthy to mention that all parameters such as  $K_s$ ,  $Y$ , and  $D$  are responsible for enhanced electrocatalytic property of n-MgF/SPE for AA detection.

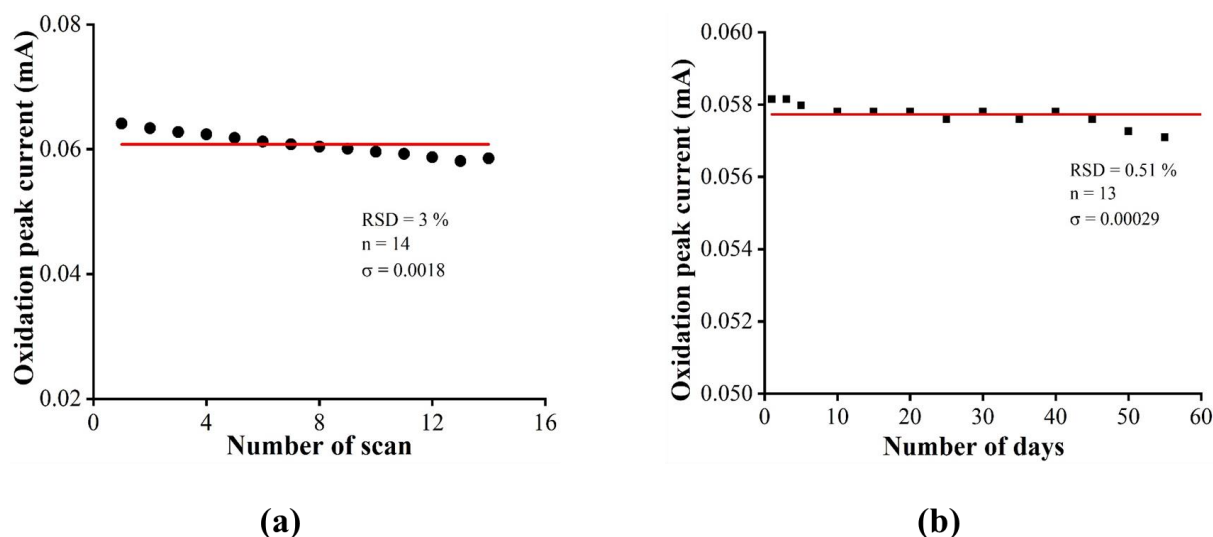


**Figure 5.8** (a) Stability analysis of n-MgF/SPE; (b) reusability analysis of n-MgF/SPE.

For the development of a sensor, we need to examine its stability as well as reusability. Stability analysis provides the information about the lifetime of a fabricated sensor. The stability analysis of the n-MgF/SPE electrode was performed in 40  $\mu$ M standard AA solution (in standard PBS) by CV technique from one to 55 days with regular interval of five days shown in **Figure 5.8** (a). After every scan, the n-MgF/SPE was stored at 4°C for further analysis. The obtained value of RSD has been found to be less than 2% after 55 days and it ensures the excellent stability of fabricated n-MgF/SPE electrode towards AA detection. Furthermore, reusability analysis was performed to confirm the testing of the AA multiple times using the same electrode. The reusability analysis of fabricated electrode was performed from one to 14 scan which shows the RSD value to be less than 2% (**Figure 5.8** (b)). Both stability and reusability analysis of the fabricated electrode confirmed that n-MgF/SPE is an excellent sensor for AA detection in real sample

#### 5.4.6 Calibration curve and interference study of n-MgF/SPE sensor for AA

In order to construct the calibration curve for AA interaction with n-MgF/SPE surface, the CV analysis was performed in the presence of standard 50 mM phosphate buffer saline (PBS, 0.9% NaCl) solution containing 5mM FRC at pH 6 with scan rate of 50 mV/s in the potential window of -0.5 to 0.5 V. The standard solution of AA was prepared in DI water covering the physiological range of AA in human body from 0 to 80  $\mu\text{M}$ . The modified n-MgF/SPE was attached with SPE holder in electrochemical transducer setup and microfluidics channel was kept on the top of modified n-MgF/SPE. The whole assembly was placed on a horizontal surface to maintain the uniform flow of standard solution of AA. 80  $\mu\text{L}$  volume of different concentration of AA solution was injected from both side of the dumbbell shaped reservoir facilitating AA to reach the detection zone. The electro-oxidation behaviour of AA towards n-MgF/SPE is represented in **Figure 5.9**.

The CV plot for different concentration of AA is depicted in **Figure 5.9** (a). It is clearly visible from **Figure 5.9** (a) that the current response decreases with increasing AA concentration in standard solution. A separate curve was plotted between change in current ( $\Delta I = I_b - I_a$ ) on y axis vs AA concentration ( $\mu\text{M}$ ) on x axis, where  $I_b$  and  $I_a$  are the values of the oxidation peak currents in absence and presence of AA respectively. A linear fitting was obtained between  $\Delta I$  and concentration ( $\mu\text{M}$ ) ( $\Delta I = 0.0004 \times \text{concentration} + 0.00285$ , linear correlation coefficient ( $R^2$ ) = 0.98). Each set of data was repeated for three times and mean value of current was taken for different concentration of AA. The obtained value of limit of detection (LOD), limit of quantification (LOQ), and sensitivity based on signal to noise ratio (S/N=3) utilising linear fitted calibration curve have been found as 2.44  $\mu\text{M}$  ( $3 \times \text{SD}/\text{slope}$ ), 8.135  $\mu\text{M}$  ( $10 \times \text{SD}/\text{slope}$ ), and  $5.71 \times 10^{-3} \text{ mA } \mu\text{M}^{-1} \text{ cm}^{-2}$  (slope/area of electrode) respectively **Figure 5.9** (b).

In the present scope of work, n-MgF/SPE was utilised for the detection of AA in real sample having various bio-analytes. Some common interfering agent such as uric acid, glutamic acid, glucose, urea, lactic acid and its mixture were mixed with standard AA solution to conduct the interference analysis on E $\mu$ PAD platform. 40  $\mu$ M concentration of different interfering agent and 80  $\mu$ M of AA were mixed and CV analysis was carried out. A bar graph plotted between different interfering agent and corresponding current values is shown in **Figure 5.9** (c). The obtained value of relative standard deviation (RSD) for different interfering agent has been found to be less than 3.85%, confirming n-MgF/SPE to be an excellent sensor for selectivity towards AA detection.

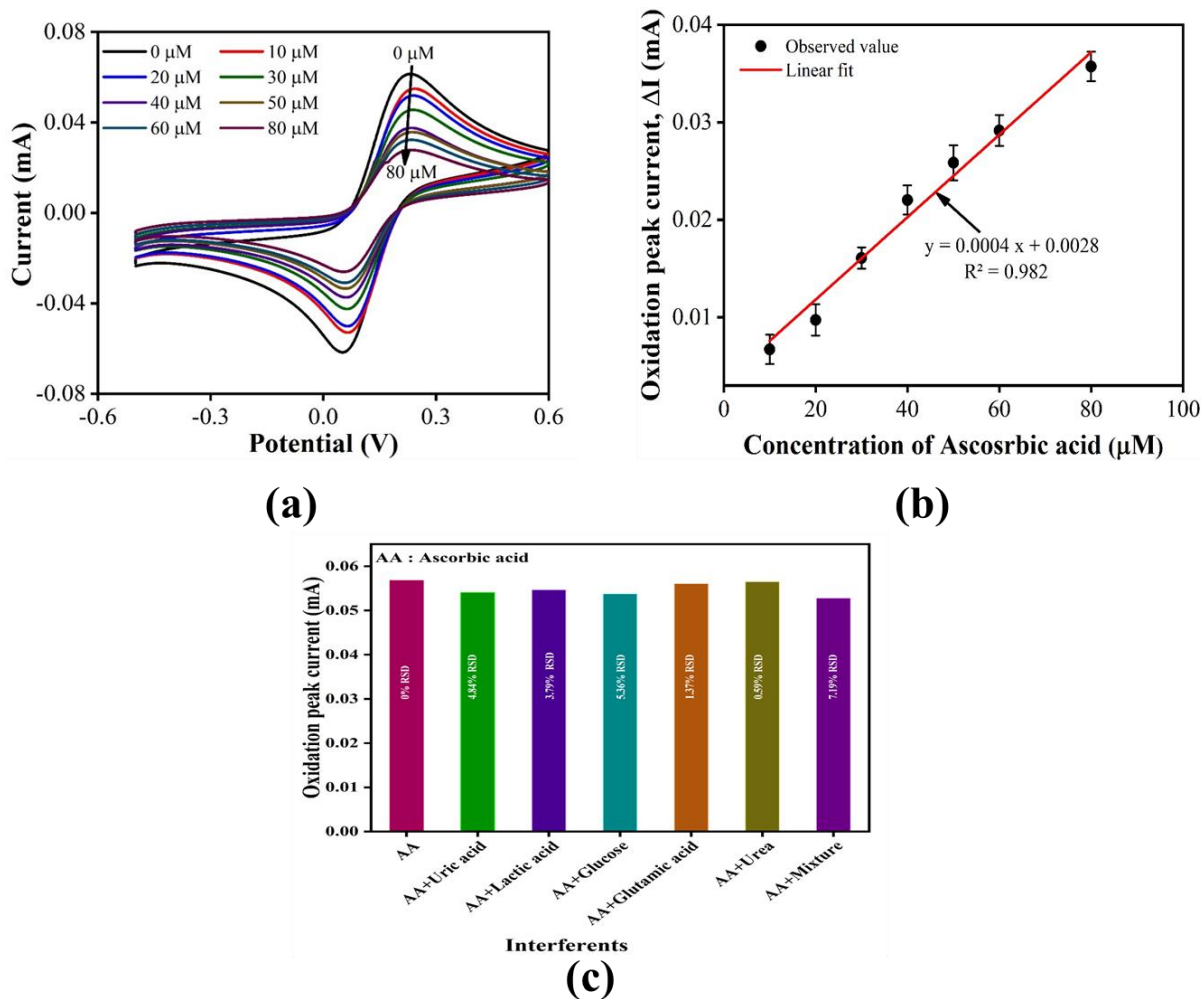


**Figure 5.9** (a) The CV plot for different concentration of AA on n-MgF/SPE; (b) A linear curve plotted between change in current ( $\Delta I = I_b - I_a$ ) on y axis vs AA concentration ( $\mu\text{M}$ ) on x-axis; (c) Interferents analysis of n-MgF/SPE.

### 5.4.7 Comparison with another developed sensor

We presented a comparison table (**Table 5-1**) to assess the performance of our developed device for ascorbic acid (AA) detection in relation to other modified screen-printed electrodes (SPEs) used for the same purpose. The data in the table reveals several advantages of our n-MgF/SPE device over the others published literature. The comparison table **Table 5-1** highlights the

superior performance of our n-MgF/SPE device in terms of its optimal linear range, excellent LOD, high sensitivity, and quick response time when compared to other modified SPE-based sensors for AA detection. Furthermore, its unique capability of integrating plasma separation with non-enzymatic electrochemical AA detection in a single step sets it apart from existing technologies in the field.

**Table 5-1** A comparison between previously reported modified SPE with our developed n-MgF sensor for AA detection.

Electrode	Method	Linear range ( $\mu\text{M}$ )	Detection limit ( $\mu\text{M}$ )	Response time (sec)	Sensitivity ( $\text{mA } \mu\text{M}^{-1} \text{cm}^{-2}$ )	Reference
PANI/SPCE	Chrono-amperometry	30-270	30	-	17.7	[164]
DBSA-doped PANI/SPE	CV	500-8000	8.3	-	-	[173]
GQDs/IL-SPCE	DPV	1.9-16.6	6.64	-	-	[172]
Au/SPE	CV/DPV	25-400	1.04	-	-	[171]
Au/SPE	DPV	1.9-16.6	-	-	$4.39 \times 10^{-6}$	[170]
$\text{Fe}_3\text{O}_4/\text{SPE}$	DPV	10-100	15.7	-	-	[162]
<b>n-MgF/SPE</b>	<b>CV</b>	<b>1-80</b>	<b>2.44</b>	<b>10</b>	<b><math>5.71 \times 10^{-3}</math></b>	<b>Present work</b>

### 5.4.8 Real sample analysis

Real sample analysis was carried out using whole human blood. A test sample with known concentration of AA (41  $\mu\text{M}$ ) was collected from hospital with test report. The test sample was spiked with 10 and 20  $\mu\text{M}$  concentration of standard AA. 80  $\mu\text{L}$  of blood sample was injected separately from both inlet reservoir of the E $\mu$ PAD to augment plasma separation and subsequently the separated plasma travel to the detection zone enabling the current signal measurement of spiked blood samples. AA concentrations of spiked blood samples were measured by utilising the calibration equation obtained from linear plot of  $\Delta I$  vs AA concentration. The measured concentration, RSD (%), and recovery values (%) were shown in **Table 5-2**.

**Table 5-2** Whole blood sample spiked with standard AA solution and concentration value measured in real spiked sample.

Sample	Spike ( $\mu\text{M}$ )	Measured ( $\mu\text{M}$ )	Recovery (%)	RSD (%)
1	0	37	93.75	6.25
2	10	52	104.20	4.20
3	20	58	97.08	2.92

## 5.5 Summary

A biodegradable non enzymatic electrochemical microfluidic paper-based device (E $\mu$ PAD) was developed for plasma separation integrated with AA detection from whole blood on the same platform via single step. The  $\mu$ PAD was fabricated by combining a blood separation membrane (LF1) and Whatman grade 1 filter paper through low-cost green wax dipping technique. n-MgF was synthesized using low-cost hydrothermal method with minimum consumption of chemical reagents. For electrochemical sensing, spherical shaped n-MgF was deposited on the SPE working area by drop-casting method. The n-MgF/SPE/E $\mu$ PAD was able to detect AA concentration in real blood samples. An interference study was carried out in the presence of some common analytes available in plasma samples such as uric acid, glutamic acid, glucose, urea, lactic acid and their mixture. The relative standard deviation (RSD) values for different interfering agent is less than 3.85%, confirming that n-MgF/SPE exhibits excellent selectivity towards AA detection in real samples. Our developed device covers the whole clinical range of plasma AA concentration with high sensitivity, lower LOD, and quick response time (10 sec). The fabricated n-MgF/SPE is stable for 55 days and reusable for 14 scans.

In our developed device whole blood is used as sample input and plasma separation occurs on same device due to the presence of 2-3  $\mu$ m pore size membrane attached at inlet section. On the same device separated plasma further travels and reach up to SPE working area section where current value is measured with the help of cyclic voltameter device. In resource limited setting this paper chip can directly be used to measure the vitamin C concentration in plasam sample with the help of small chip. For further improvement three electrode system can be directly printed of the paper substrate to measure the current variation due to change in AA concentration in whole blood sample.

Overall, the biodegradable, non-enzymatic E $\mu$ PAD we have developed offers a cost-effective, user-friendly solution for simultaneous plasma separation and AA detection from whole blood in a single step. Its high selectivity, sensitivity, and stability make it a promising tool for point-of-care applications.

